RSC Advances

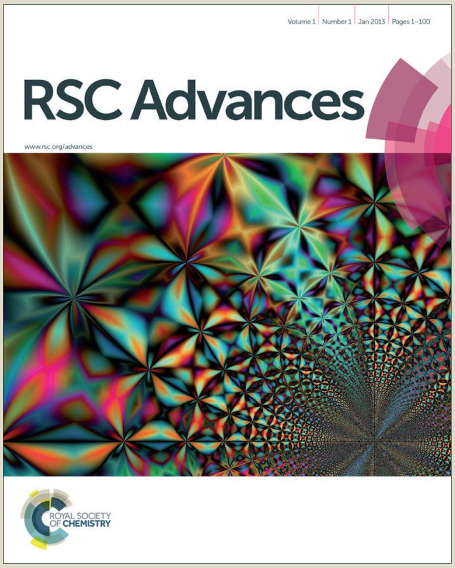

ROYAL SOCIETY
OF CHEMISTRY

www.rsc.org/advances

Journal Name

COMMUNICATION

GaN nanorod array as precursor to enhance GaN:Mn Ferromagnetism

Received 00th January 20xx,
Accepted 00th January 20xx

DOI: 10.1039/x0xx00000x

www.rsc.org/

Cheng Ji,[a] Shengxiang Jiang,[a] Yan Zhang,[b] Haiyin Xing,[c] Zhijian Yang,[a] Cunda Wang,[a] Tongjun Yu[a,†] and Guoyi Zhang[a,†]

With a high surface-to-volume ratio, Ga-polar GaN nanorod array was designed and realized as the precursor to grow ferromagnetic enhanced GaN:Mn film by MOCVD. HRXRD and Raman scattering results might imply a correlation between the ferromagnetism in GaN:Mn and the built-in defects in intrinsic GaN lattice induced when Mn doping was applied.

Nanorod, as a one-dimensional nanostructure, has the uniqueness of large surface-to-volume ratio, dislocation reducing, strain relieving, and it is commonly recognised that nanorod array produced on standard size substrate is applicable for industrial use. Therefore, many theoretical and applied research have been done based on this kind of material and its derivatives.[1-3] However, much of the attention is thrown to the aspect of high crystal quality or low dimension, and many other interesting nanorod-induced features remain to be investigated.

Under the spintronic idea of simultaneously manipulating both the spin and charge of carriers in devices, diluted magnetic semiconductors (DMSs) have entered people's vision as a fundamental spin injection material.[4] And DMSs like GaMnAs and InMnAs have been made and applied in many spintronic research.[5] However, an industrial use of DMSs requests a high transition temperature and a distinct magnetic feature. Based on GaN:Mn's promising high transition temperature in the spin part and, moreover, the wide application of GaN in the charge part, GaN:Mn becomes appealing in the pursuit of practical spintronic devices.[6,7] And high-temperature ferromagnetic GaN:Mn has been reported in both films[8-10] and nano structures[11,12]. Therefore, the idea of nanorod array based ferromagnetic GaN:Mn begins to catch the attention of researchers. And recently, Lin *et al.* have, for the first time, successfully produced above room-temperature ferromagnetic GaN:Mn nanorod array with MBE.[13]

On the other hand, the new features induced by nano structure in itself are also new subjects for DMS theory. As the guidance on finding DMSs with high transition temperature and strong ferromagnetism, the theoretical understanding of the ferromagnetism in DMSs is in great demand. However, this problem, which was always based on conventional DMS film structure in previous research, has been a subject of lengthy debate.[14,15] Against this background, a new structure may provide us a new perspective on this problem.

In this work, we suggested that GaN nanorod array has the potential to be a good precursor in producing GaN:Mn with enhanced ferromagnetism, and used Ga-polar GaN nanorod array to grow high-temperature ferromagnetic GaN:Mn film. As was hoped, the saturation magnetization and residual magnetization in this structure were distinctly enhanced, compared to conventional GaN:Mn films. High-resolution X-ray diffraction (HRXRD) and Raman scattering excluded the possibility of micro-precipitates or clusters. They also implied a correlation between the ferromagnetism in GaN:Mn films and the built-in defects in intrinsic GaN lattice induced with Mn doping.

The strategy of nano-precursor showed a way to enhance ferromagnetism in DMS by the control of defects. And the material itself supported the idea that the defect caused by the process of growth plays an important role in the magnetism in DMS system. Moreover, the ferromagnetic enhancement caused by nanorod precursor also showed a new train of thought that, not just a nano structure itself has interesting phenomena, when acting as a precursor, it can also bring the marvels of nano world into macroscopic bulk materials.

As indicated in many works, defects like V_{Ga}, V_N, or N split may play an important role in the ferromagnetism of GaN:Mn film.[16-19] Though their views on the defect type are diverse, point defect is a consensus. According to this philosophy, we suppose, if we intentionally induce more point defects in a GaN:Mn structure, we might be able to get a magnetic

---

[a] *Research Center for Wide Gap Semiconductors, State Key Laboratory for Artificial Microstructure and Microscopic Physics, School of Physics, Peking University, 100871 Beijing, PR China.*
[b] *Institute of condensed matter physics, School of Physics, Peking University, 100871 Beijing, PR China.*
[c] *School of Electronics and Information Engineering, Tianjin Polytechnic University, Tianjin 300387, China*
† Email: *tongjun@pku.edu.cn, gyzhang@pku.edu.cn.*

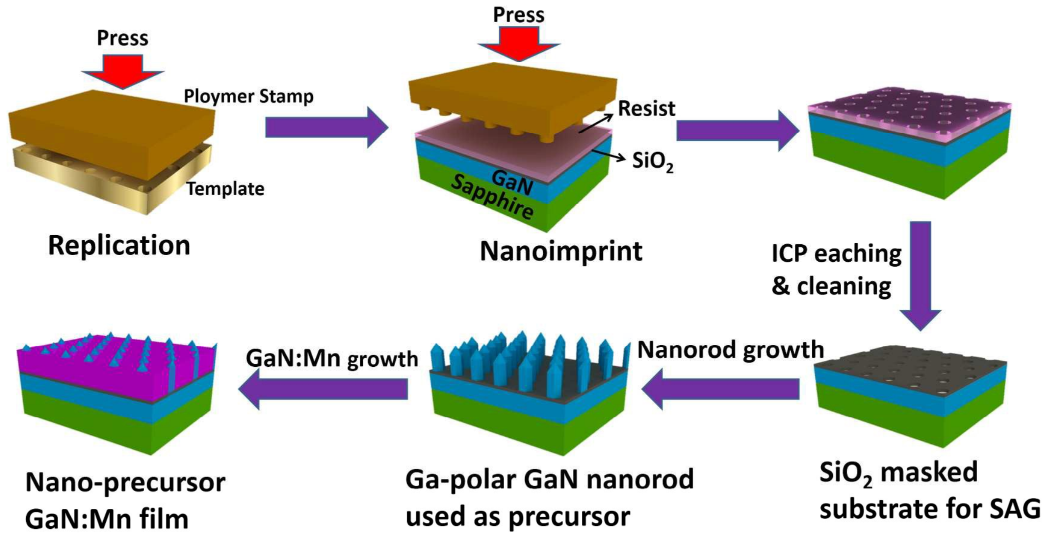

Fig. 1 (coloured online) The process of producing our nano-precursor GaN:Mn film.

enhanced GaN:Mn material.

With a large surface to volume ratio, nanorod array can provide a large amount of coalescence boundary when grown into a film. These boundaries usually cause a high density of threading dislocations; and a lot of point defects can be induced along with the threading dislocations. Therefore, nanorod array has the potential to be a good precursor in producing GaN:Mn with enhanced ferromagnetism.

The whole process of our sample preparation is shown in Fig. 1. The substrate for GaN nanorod growth was a layer of 3 um c-plane GaN on sapphire capped with 50 nm SiO_2 mask layer; this substrate was prepared by nano-imprinting lithography (NIL) with an Obducat Eitre3 instrument and by inductively coupled plasma (ICP) dry etching with a Samco RIE-200ip etcher. The process of preparing this substrate is similar to previous works in our group.[20]

The SiO_2 mask provided a pitch 500 nm and diameter 200 nm hexagonal arranged hole pattern for nanorod selective area growth (SAG),[1] and then GaN nanorod array was grown in a Thomas Swan close coupled showerhead reactor metal organic chemical vapor deposition (MOCVD) system. The GaN nanorod array was grown 300 nm high with a direct nanorod growth with 136 μmol/min TMGa, 160 sccm NH_3 and 1 sccm SiH_4. The substrate temperature was 1068℃ and the reactor pressure was 300 mbar.

Both N-polar (grown directly from sapphire under the SiO_2 mask) and Ga-polar nanorod arrays were made, and used as the precursor for GaN:Mn film. It turned out that, only the nanorod array from Ga-polar growth could be used as the precursor for successive GaN:Mn growth, while the N-polar nanorod array could not. This difference could be clarified by the SEM (Nova Nano SEM 430) observation of morphology shown in Fig. 2(a) and (b). Nanorod array from Ga-polar growth resulted in a pyramidal top, while that from N-polar growth formed a top part having the shape of a truncated pyramid or even just a flat top, which means a closed r-plane in N-polar nanorod array.[21]

After the Ga-polar nanorod array was made, it was grown into a 450nm thick GaN:Mn film in 5.64 μmol/min TMGa, 0.87 μmol/min $(MCP)_2Mn$, 25 sccm NH_3 and 1 sccm SiH_4, as shown in Fig. 2(c). This time, the substrate temperature was 1020℃ and the reactor pressure was 100 mbar. As for the conventional ferromagnetic GaN:Mn film which is used for comparison here, it was grown directly from c-plane GaN film on sapphire. This was performed under 1060℃, 100 mbar and a source flow of 11.28 μmol/min TMGa, 1.73 μmol/min ($(MCP)_2Mn$) and 4.8 slm NH_3. All the GaN:Mn growth was done

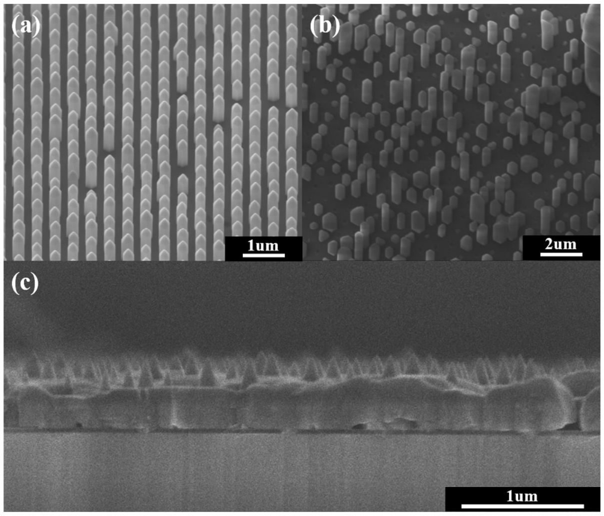

Fig. 2 SEM image of (a) Ga-polar GaN nanorod array (45° tilted) (b) N-polar GaN nanorod array (45° tilted) (c) the nano-precursor GaN:Mn film (cross section).

in a low pressure horizontal reactor MOCVD system. The Mn concentration of the GaN:Mn film was controlled by varying the ratio of the molar flow of Mn and Ga going into the reactor and, to freeze more Mn atoms in the GaN lattice, a high V/III ratio and ultra-fast cooling was applied in GaN:Mn growth.[8] The film with 2.8% Mn content was found to have the most significant ferromagnetic feature in the nano-precursor GaN:Mn film, so a 2.8% Mn doping conventional GaN:Mn film was grown for comparison.

Hysteresis loops were measured to characterise the magnetism of the GaN:Mn films. As the magnetic signals for most magnetic semiconductors, including the GaN:Mn film, are usually weak, a very careful operation and a measurement as sensitive as possible were performed to obtain reliable data.[22] The magnetization was measured in the most sensitive RSO mode in a commercial superconducting quantum interference device (SQUID) magnetometer MPMS XL from Quantum Design, and the result is shown in Fig. 3.

In bare GaN nanorod array and GaN film, only diamagnetic background assigned to sapphire substrate could be seen (not shown in Fig. 3). The hysteresis loops of the nano-precursor GaN:Mn film at 30K, 150K and 300K were measured with the external magnetic field parallel to the surface of the film. The result indicated an above room-temperature ferromagnetism in the nano-precursor GaN:Mn film, which is similar to the result in conventional GaN:Mn film.[8] The slowly decrease of saturation magnetizations when temperature increases could be explained by thermal motion of domains.

A comparison with conventional GaN:Mn film shows a 2.5 times increment from 0.86 emu/cm^3 to 2.14 emu/cm^3 in saturation magnetization. The inset is an enlarged image of the zero field part of the hysteresis loops; and it shows a significant more-than-three-time increment from 0.08 emu/cm^3 to 0.26 emu/cm^3 in residual magnetization. Also, the coercivity increases from 80 Oe to 115 Oe, which is not so significant, but much larger than their nano counterparts of about 35 Oe.[11,13] These results favourably support our nano-precursor hypothesis that a GaN:Mn structure with more point defects might result in magnetic enhancement.

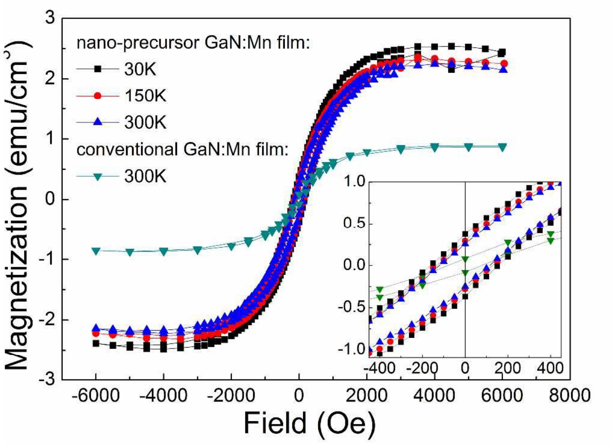

Fig. 3 (coloured online) Hysteresis loops of the nano-precursor GaN:Mn film at 30K (square), 150K (dot) and 300K (up triangle), and conventional GaN:Mn film at 300K (down triangle). Inset: enlarged image of the zero field part of the hysteresis loops.

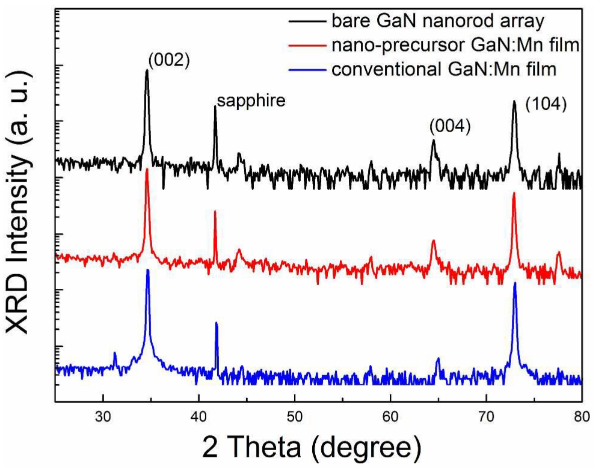

Fig. 4 (coloured online) HRXRD ω–2θ scan curves for bare GaN nanorod array, the nano-precursor GaN:Mn film and conventional GaN:Mn film.

High-resolution X-ray diffraction (HRXRD: Bruker D8) was used to analyse the structure of the samples. As for the ω–2θ scan curves shown in Fig. 4, peaks at 31.1^{o}, 34.5^{o}, 64.8^{o}, 72.9^{o} and 41.8^{o}, responding to GaN (100), (002), (103), (004) face and sapphire, occur in all the spectra.[23] Peaks at 44.2^{o}, 57.8^{o} and 77.5^{o} occur only in the nano-precursor GaN:Mn film and bare GaN nanorod array, which are induced by the amorphous SiO$_2$ mask layer.[24] No additional peak from Mn-related secondary phases or impurities appears in either the Mn-doped GaN films. This result indicated that this kind of ferromagnetic GaN:Mn film is in a single phase, which is similar to the results in our previous works on conventional GaN:Mn films.[8]

Also, compared with bare GaN nanorod array and conventional GaN:Mn film under the same level of Mn doping, the rocking curves of the nano-precursor GaN:Mn film were measured on (002) and (102) planes. It was found that the full width at half maximums (FWHM) on (002) plane were 281 arcsec for the nano-precursor GaN:Mn film, 314 arcsec for conventional GaN:Mn film and 270 arcsec for bare GaN nanorod array. This decrease in nanostructure and nano-precursor could be understood as the result of strain releasing in nanorod growth.[25] As for the FWHMs on (102) plane, the nano-precursor GaN:Mn film was 315 arcsec, the conventional GaN:Mn film was 314 arcsec, and the bare GaN nanorod array was 309 arcsec. There was not a distinct difference among these three. Given that the (002) and (102) plane FWHM always relate to screw dislocations and edge dislocations respectively, the results implied the threading dislocation might not be responsible to the ferromagnetic enhancement.[25]

We also carried out a preliminary hall test with the three samples. The Ti/Al/Ni/Au (25/120/45/100nm) electrodes were made at the four corners of a 1×1 cm^2 square, followed by a 30s rapid thermal annealing at 830℃ in N_2 atmosphere to form ohmic contact. The measurement was performed with an Accent HL5500 Hall measurement system. Compared with the conventional GaN:Mn film, the nano-precursor GaN:Mn film showed a smaller mobility and a significantly higher carrier concentration. On one hand, the decrease in mobility could be explained by more defect scattering. On the other, the remarkable increase in carrier concentration might be caused by the increase in donor-like point defects. Though further works like deep-level transient spectroscopy (DLTS) need to be done to identify the species of the point defect, these results might imply more point defects in our nano-precursor GaN:Mn film.

Fig. 5 shows the result of Raman scattering (Renishaw Confocal Raman microscope) at room temperature. The spectra of bare GaN nanorod array and conventional GaN:Mn film are also shown for comparison. The peaks at 570 cm^{-1} and 735 cm^{-1} are assigned to the E_2^H and A_1(LO) phonon modes respectively. Unlike previous works in room-temperature ferromagnetic GaN:Mn in both films and nanostructures, we did not find any shoulder peak of E_2^H peak at about 588 cm^{-1}, which is always assigned to Mn-N pairs, micro-precipitates or clusters in any of these Raman spectra.[13,26-28] Considering the small amount of Mn in both the ferromagnetic GaN:Mn films, the Mn amount or other forms of cluster may not be the most critical factor for the ferromagnetism in GaN:Mn material. This is also a side evidence of uniform magnetization in the GaN:Mn films.

A small Raman peak at 671 cm^{-1} occurs in both conventional GaN:Mn film and the nano-precursor GaN:Mn film. But it doesn't appear in bare GaN nanorod array or conventional GaN film. This difference means that the 671cm^{-1} Raman mode was induced with Mn doping. This behaviour in Raman spectrum was also observed when implanting other magnetic ions into GaN, and it has nothing to do with ionic species.[29] This result implied, not to the substituting impurities themselves, this ferromagnetism related 671 cm^{-1} Raman mode is assigned to disorder activated Raman scattering of built-in defects in intrinsic GaN lattice. Consistent with the results from XRD and the Hall measurement, the results implied that the high-temperature ferromagnetism of GaN:Mn film may relate to the built-in defects in intrinsic GaN lattice.

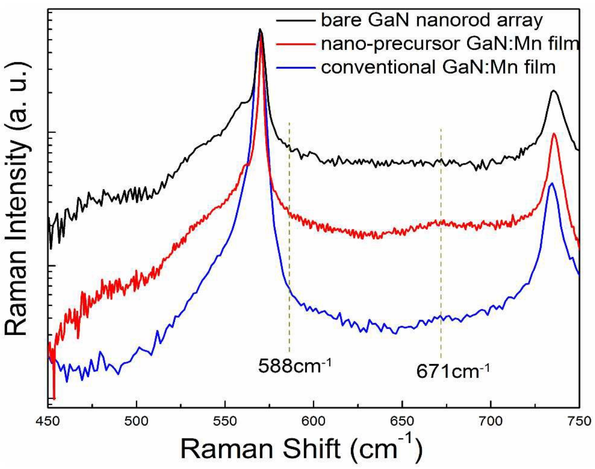

Fig. 5 (coloured online) Raman spectra of bare GaN nanorod array, the nano-precursor GaN:Mn film and conventional GaN film.

Conclusions

In conclusion, we took the advantage of high surface-to-volume ratio of nanorod array, and pointed out it has the potential to be a precursor in producing GaN:Mn with enhanced ferromagnetism with a defect control. Hereby, 2.8% GaN:Mn film was grown from Ga-polar GaN nanorod array as the precursor in MOCVD. And as was hoped, the film had a high-temperature ferromagnetism, and a significant magnetic enhancement compared with its conventional counterpart. HRXRD and Raman results excluded the possibility of micro-precipitates and clusters, and related the critical reason for ferromagnetism in GaN:Mn to the built-in defects in intrinsic GaN lattice induced with Mn doping. Moreover, the strategy of nano-precursor showed a way to enhance ferromagnetism in DMS, and provided a new train of thought for nano application in macroscopic world.

Acknowledgements

The work was supported by the National Key Basic Research Special Foundation of China under grant No. 2013CB328705, No.2011CB013101 and National Natural Science Foundation of China under Grant No. 61327801, No. 61376012, No. 61204008.

Notes and references

1 S. Li and A. Waag, *Journal of Applied Physics*, 2012, **111**, 071101.
2 M. Tchernycheva, V. Neplokh, H. Zhang, P. Lavenus, L. Rigutti, F. Bayle, F. H. Julien, A. Babichev, G. Jacopin, L. Largeau, R. Ciechonski, G. Vescovi and O. Kryliouk, *Nanoscale*, 2015, **7**, 11692-11701.
3 Y.-T. Lin, T.-W. Yeh, Y. Nakajima and P. D. Dapkus, *Advanced Functional Materials*, 2014, **24**, 3162-3171.
4 I. Žutić, J. Fabian and S. Das Sarma, *Reviews of Modern Physics*, 2004, **76**, 323-410.
5 D. D. Awschalom, Y. Ohno, D. K. Young, B. Beschoten, F. Matsukura and H. Ohno, *Nature*, 1999, **402**, 790-792.
6 T. Dietl, *Science*, 2000, **287**, 1019-1022.
7 K. Sato and H. Katayama-Yoshida, *Japanese Journal of Applied Physics*, 2001, **40**, L485-L487.
8 C. Zhi-Tao, S. Yue-Yong, Y. Zhi-Jian, Z. Yan, Z. Bin, G. Li-Ping, X. Ke, P. Yao-Bao, Z. Han and Z. Guo-Yi, *Chinese Physics Letters*, 2006, **23**, 1286-1288.
9 M. L. Reed, N. A. El-Masry, H. H. Stadelmaier, M. K. Ritums, M. J. Reed, C. A. Parker, J. C. Roberts and S. M. Bedair, *Applied Physics Letters*, 2001, **79**, 3473.
10 F. Zhang, N. Chen, X. Liu, Z. Liu, S. Yang and C. Chai, *Journal of Crystal Growth*, 2004, **262**, 287-289.

11 H. J. Choi, H. K. Seong, J. Chang, K. I. Lee, Y. J. Park, J. J. Kim, S. K. Lee, R. He, T. Kuykendall and P. Yang, *Advanced Materials*, 2005, **17**, 1351-1356.
12 Y. P. Song, P. W. Wang, X. H. Zhang and D. P. Yu, *Physica B: Condensed Matter*, 2005, **368**, 16-24.
13 Y. T. Lin, P. V. Wadekar, H. S. Kao, T. H. Chen, H. C. Huang, N. J. Ho, Q. Y. Chen and L. W. Tu, *Applied Physics Letters*, 2014, **104**, 062414.
14 T. Dietl, *Nat Mater*, 2010, **9**, 965-974.
15 M. E. Flatté, *Nature Physics*, 2011, **7**, 285-286.
16 B. Hu, B. Y. Man, M. Liu, C. Yang, C. S. Chen, X. G. Gao, S. C. Xu, C. C. Wang and Z. C. Sun, *Applied Physics A*, 2012, **108**, 409-413.
17 G. Thaler, R. Frazier, B. Gila, J. Stapleton, M. Davidson, C. R. Abernathy, S. J. Pearton and C. Segre, *Applied Physics Letters*, 2004, **84**, 2578.
18 D. J. Keavney, S. H. Cheung, S. T. King, M. Weinert and L. Li, *Physical Review Letters*, 2005, **95**, 257201.
19 X. L. Yang, Z. T. Chen, C. D. Wang, S. Huang, H. Fang, G. Y. Zhang, D. L. Chen and W. S. Yan, *Journal of Physics D: Applied Physics*, 2008, **41**, 125002.
20 S. X. Jiang, Z. Z. Chen, X. Z. Jiang, X. X. Fu, S. Jiang, Q. Q. Jiao, T. J. Yu and G. Y. Zhang, *CrystEngComm*, 2015, **17**, 3070-3075.
21 S. F. Li, S. Fuendling, X. Wang, S. Merzsch, M. A. M. Al-Suleiman, J. D. Wei, H. H. Wehmann, A. Waag, W. Bergbauer and M. Strassburg, *Crystal Growth & Design*, 2011, **11**, 1573-1577.
22 M. Sawicki, W. Stefanowicz and A. Ney, *Semiconductor Science and Technology*, 2011, **26**, 064006.
23 H. Xiao, R. Liu, H. Ma, Z. Lin, J. Ma, F. Zong and L. Mei, *Journal of Alloys and Compounds*, 2008, **465**, 340-343.
24 M. B. Boisen, G. V. Gibbs and M. S. T. Bukowinski, *Physics and Chemistry of Minerals*, 1994, **21**, 269.
25 W. C. Yang, K. Y. Chen, K.-Y. Cheng, Y. L. Wang, K. C. Hsieh and K. Y. Cheng, *Journal of Crystal Growth*, 2015, **425**, 141-144.
26 X. Yang, J. Wu, Z. Chen, Y. Pan, Y. Zhang, Z. Yang, T. Yu and G. Zhang, *Solid State Communications*, 2007, **143**, 236-239.
27 X. Q. Xiu, R. Zhang, B. B. Li, Z. L. Xie, L. Chen, B. Liu, P. Han, S. L. Gu, Y. Shi and Y. D. Zheng, *Journal of Crystal Growth*, 2006, **292**, 212-215.
28 M. Asghar, I. Hussain, E. Bustarret, J. Cibert, S. Kuroda, S. Marcet and H. Mariette, *Journal of Crystal Growth*, 2006, **296**, 174-178.
29 W. Limmer, W. Ritter, R. Sauer, B. Mensching, C. Liu and B. Rauschenbach, *Applied Physics Letters*, 1998, **72**, 2589.